Journal of Non-Crystalline Solids 147&148 (1992) 296–302
North-Holland

JOURNAL OF
NON-CRYSTALLINE SOLIDS

Processing of silica xerogels using sonocatalysis and an additive

E. Blanco, N. de la Rosa-Fox and L. Esquivias
Departamento de Estructura y Propiedades de los Materiales, Facultad de Ciencias, Universidad de Cádiz, Cadiz, Spain

A.F. Craievich
Laboratorio Nacional de Luz Sincrotron / CNPq, Campinas, SP, Brazil, and Instituto de Física / USP, Sao Paulo, Brazil

Drying control chemical additives (DCCA) can be used to obtain monolithic glasses. Processing steps are unclear or not well known. This work studies the processing of xerogels prepared with formamide as an additive, tetraethoxysilane (TEOS) and acid water in a molar ratio of 7:1:10, respectively, with high power ultrasound. In order to calculate the evolution of the main ultrastructural parameters, the entire processing has been followed by small-angle X-ray scattering (SAXS) and nitrogen adsorption–desorption isotherms.

1. Introduction

The sol–gel method, widely used to obtain monolithic silica glasses, is particularly useful because of its great potential to produce complex-shaped glasses [1], advanced materials such as fibres [2] and graded refractive index glasses [3]. The drying stage of this process removes the interstitial liquid of the pores. This is a delicate step in this processing in order to prevent gel fragmentation [4]. Gel cracking during drying is a consequence of the stresses produced by capillary forces associated with the gas–liquid interfaces within the pores [5]. One method used to avoid the gel fracture consists of suppressing the liquid–gas interface under hypercritical conditions [6], and then sintering the 'aerogel' to produce monolithic glasses [7].

Another approach consists of the addition of a drying control chemical additive (DCCA) in the liquid state before gelling [8]. Formamide is one of the most common DCCAs used for this purpose. It seems that this additive forms a layer on the gel surface, protecting it against gel cracking [9]. Porosity evolution after drying and the shrinkage rate of such xerogels under controlled heats treatments are not well known.

It is useful to combine sonocatalysis and formamide to obtain monolithic xerogels [10], in order to vary their structural characteristics. This work is an attempt to optimize the different relevant parameters involved in the monolithic xerogels processing.

2. Experimental

2.1. Preparation of xerogels

Silica gels were prepared from tetraethoxysilane (TEOS) hydrolyzed by HNO_3 acid water ($pH = 1$) and formamide as an additive, in a molar ratio 1:10:7, respectively.

Sonogels [11] have been prepared by the application of high power ultrasound (HPU), at 20 kHz, to the mixture. The HPU processor has 600 W as power output and a standard horn with a 9.5 mm tip. When ultrasound energy is applied to the liquid, it is necessary to know the power which has been supplied to the reaction. A calibration of our ultrasonic processor was carried out by the measurements of the temperature increases for several water volumes and different power levels. Temperature versus time plots were

0022-3093/92/$05.00 © 1992 – Elsevier Science Publishers B.V. All rights reserved

obtained. For each power level, the graphs exhibit a linear region whose slope is the energy supplied to the liquid. It is then possible to know the power supply for different liquid volumes when a given ultrasound power level is selected in the processor. Two different ultrasound energies were used, a low and high ultrasound dose of 0.1 and 0.3 kJ, respectively.

Sols obtained by this way were kept in hermetically closed polyethylene containers. The gelation took place in an electric oven at 40°C. After 7 days aging, containers were opened and the samples were dried at 40°C until the liquid was completely evaporated.

2.2. Heat treatments

A first heat treatment was carried out at 100°C for 24 h in an electric oven. During this stage, monolithic xerogels shrink and their volume is reduced about 50% with a final bulk density of 1.0 g/cm^3. Then gels were introduced in a programmable electric furnace and subjected to different isothermal heat treatments at 200, 400, 600 and 800°C. For each heat treatment, the starting samples were different pieces of the same xerogel stored in the oven at 100°C. Samples were removed from the furnace at different time intervals which are indicated in table 1. Samples heat treated above 500°C were chlorinated with a CCl_4 flow during 10 h. The heating rate was 0.5°C/min in all cases.

Thermal gravimetric analysis (TGA) was carried out during an isothermal treatment at 200°C after heating at 1°C/min. At TGA at constant rate heating was performed at 10°C/min from 25 to 1000°C.

Table 1
Xerogels preparation conditions and heating time

Sample	Ultrasonic energy (kJ)	Temperature (°C)	Heating time (min)
H21	0.3	200	60
H210	0.3	200	600
H61	0.3	600	60
H84	0.3	800	240
L210	0.1	200	600
L41	0.1	400	60
L429	0.1	400	1800
L61	0.1	600	60

Gels were sintered to glass at a constant heating rate of 1°C/min, after an isothermal heating at 200°C for 10 h without chlorination. Raman spectroscopy was used to follow the gel–glass transformation on sintering.

2.3. Nitrogen physisorption measurements

The pore analysis was carried out in a noncommercial high vacuum device with nitrogen gas as adsorbate. Pressures were measured using a MKS captor model BHS 1000 with a pressure-range of 0–1000 Torr. Samples were first degassed to empty the pores. The apparent chamber volume was measured with helium gas. Afterwards, equilibrium pressures of adsorbed and desorbed nitrogen were determined. The adsorbed and desorbed nitrogen volumes were obtained from the pressures, the apparent chamber volume and prechamber volume. The S_{BET} is calculated for $P/P < 0.35$ and pore volume from the nitrogen V_{ads} at $P/P_0 \approx 1$.

Pore size distribution was calculated using the Kelvin [12] equation in the form

$$\frac{1}{r_1} + \frac{1}{r_2} = -\frac{RT}{\sigma V} \ln\left(\frac{P}{P_0}\right). \qquad (1)$$

Equation (1) relates the principal curvature radii, $r_1 y r_2$, of the liquid meniscus in the pore to the relative pressure, P/P_0, at which condensation occurs; σ is the surface tension of the condensed liquid and V is its molar volume. It is generally assumed that this equation can be applied locally to each element of the liquid surface.

This approach to obtain the pore radius holds under the conditions that a geometrical model for the pore shape is assumed and the curvature of the meniscus is directly related to the pore width. The pore shape is assumed to be either cylindrical or slit-shaped. In the former case, the meniscus is hemicylindrical and $r_1 = r_2$, while in the latter case the meniscus is hemicylindrical, $r_1 =$ width of slit and $r_2 = \infty$. When the Pierce method is used, as in this case, the first hypothesis is considered [13] and the r_k value is obtained from eq. (1). This r_k value corresponds to the pore radius in which condensation occurs at the required relative pressure.

If the radius of a cylindrical pore is r_p and a correction is made for the thickness of a layer already adsorbed on the pore walls, it is necessary to obtain a parameter t, called multilayer thickness, which permits the calculation of r_p from r_k by $r_p = r_k + t$. The t-values are experimentally obtained from the adsorption data of a non-porous pure silica sample.

2.4. SAXS measurements

Small angle X-ray scattering (SAXS) experiments were carried out using the LURE synchrotron radiation facility at Orsay, France. A very intense monochromatic 8 keV X-Ray beam with point-like cross-section was used. SAXS spectra have been measured with a 18 cm one-dimensional position sensitive detector located at 1 m from the sample. SAXS intensity was measured as a function of the modulus of the scattering vector, $q = 4\pi \sin(\theta/\lambda)$, θ being half of the scattering angle and λ the X-ray wavelength (0.01 $A^{-1} \leq q \leq 0.67$ A^{-1}). Background noise was subtracted after recording two scattering curves, one with the sample in the holder and the other one without the sample. An ionization chamber behind the sample was used to monitor the monochromatic direct beam intensity to normalize the SAXS plots. A vacuum tube was used between sample and detector to suppress air scattering.

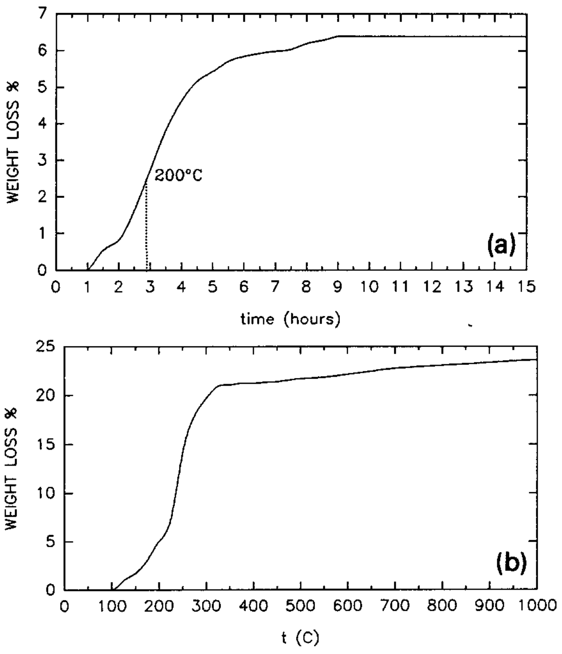

Fig. 1. TGA curves. (a) Isothermic treatment: after 6 h it can be considered that all the formamide have taken off the pores. (b) Low dose sample TGA up to 1000°C: most of the weight losses corresponding to organic residue removal take place between 230 and 330°C.

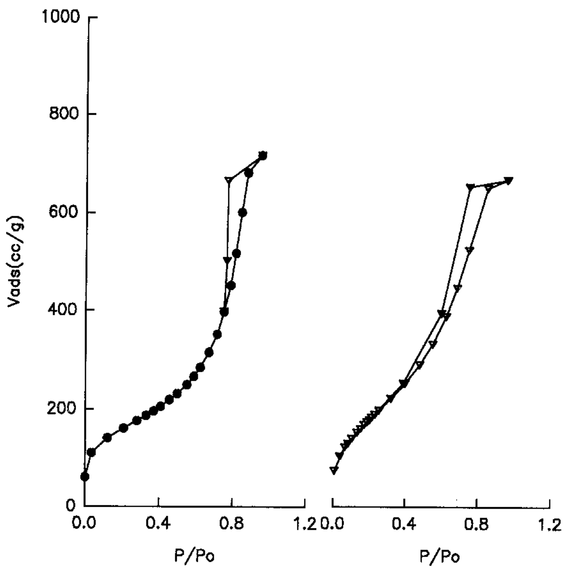

Fig. 2. Type IV isotherm obtained from nitrogen physisorption for H61 (left) and H84 (right) samples. It can be inferred from the loop shapes these xerogels are formed by agglomerates of uniform sphere-like particles.

3. Results

Figures 1(a) and (b) show TGA corresponding to a low ultrasound dose silica gel according to the above described procedure. As can be seen, there is no further weight loss after 6 h of isothermal heating at 200°C. Taking into account the formamide boiling point (below 200°C), it is considered that the additive has been completely

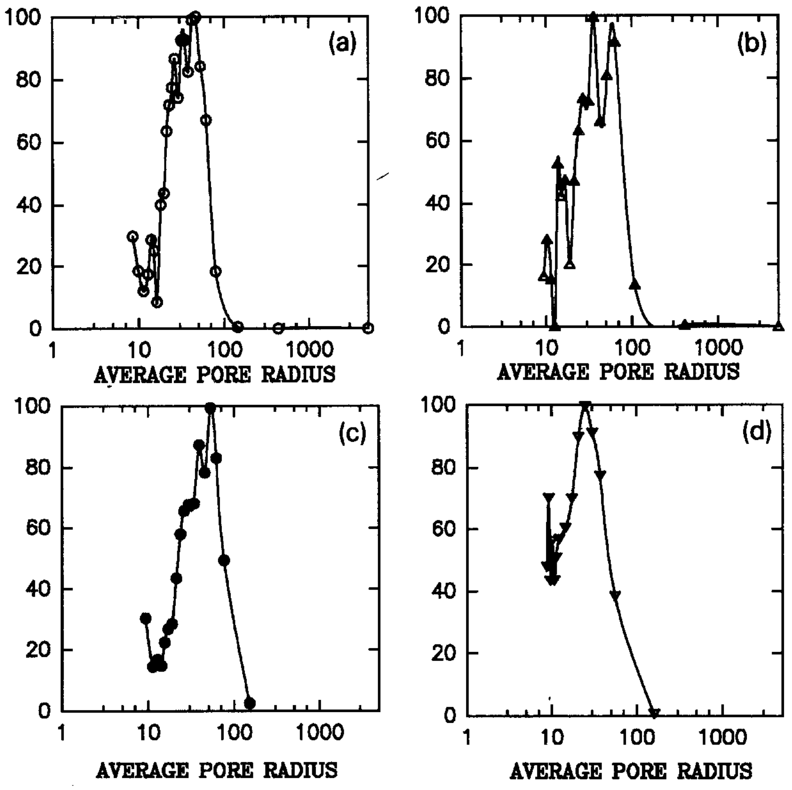

Fig. 3. Pore size distribution. Pore radius versus dV/dr of: (a) ○, a L210; (b) △, L41; (c) •, H61; (d) ▽, H84. In all cases, a 40 Å main pore size appears except in that heat treated at 400°C where two maxima (at 40 Å and 70 Å) can be observed.

removed from the pores. Constant rate heating shows that the most important weight loss occurs over the 230–830°C temperature range and it is due to organic radicals departing from the gel surface.

All physisorption isotherms obtained (fig. 2) are type IV with hysteresis loops which are associated with capillary condensation in mesopores and the limiting uptake over P/P_0 close to 1. The hysteresis loop shapes have often been identified

Table 2
Some textural parameters of studied xerogels

Sample	ρ_a (g cm^3)	S_{BET} (m^2 g^{-1})	r_a (Å)	r_θ (Å)	$N+1$	V_p (cm^{-3}/g)	V_p^* (cm^{-3}/g)	r_p/r_a
H21	0.67	722	45.6	11.7	21	1.27	0.94	0.72
H210	0.62	741	45.6	11.2	23	1.29	1.00	0.77
H61	0.60	544	50.5	11.4	25	1.11	1.13	0.81
H84	0.69	649	62.8	8.5	128	1.03	0.97	0.50
L210	0.62	715	47.5	14.2	11	1.18	1.09	0.77
L41	0.60	538	54.8	14.6	15	1.23	1.15	0.83
L429	0.63	511	50.5	15.7	11	1.12	0.92	0.87
L61	0.64	592	47.1	11.4	22	1.03	1.01	0.74

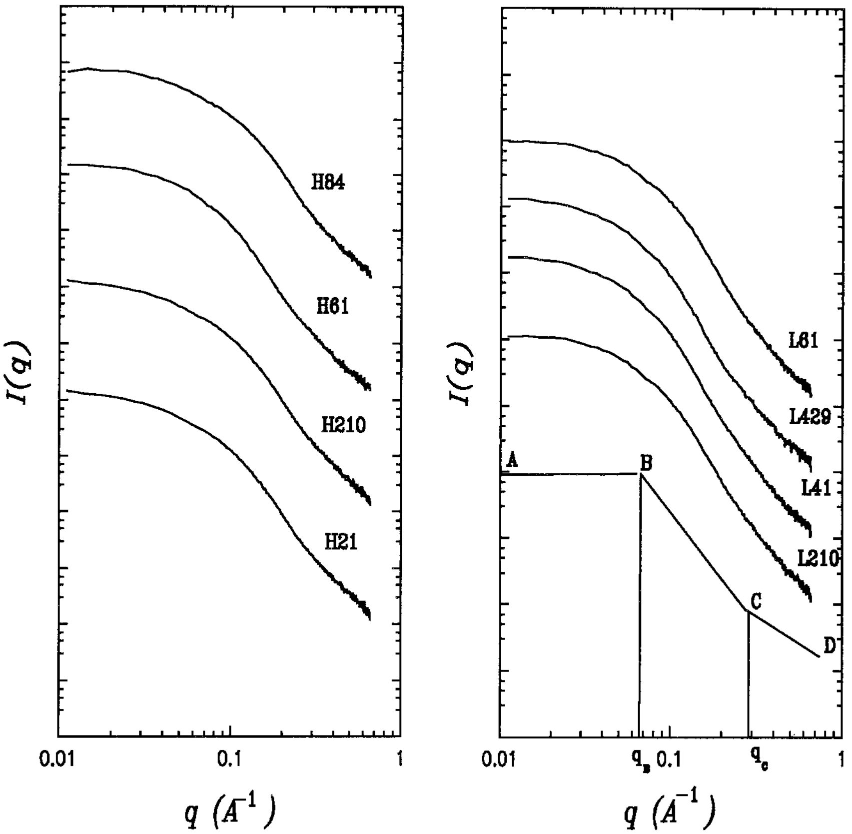

Fig. 4. SAXS log–log plots for high (left) and low (right) energy series. An aggregation index is calculated from the quotient of the crossover points q_C / q_B (see text).

with specific pore structures. In this case, it is possible to consider the loop shapes between H1 and H2 * types. Then, it is assumed that the xerogels consist of agglomerates or compacts of approximately uniform spheres in fairly regular array.

Figure 3 shows pore size distribution for some xerogels. In all cases, it is possible to establish a main pore radius of 40 Å which corresponds to the maximum of the distribution. There is only one temperature, 400°C, where different maxima can be clearly observed at approximately 40 Å, as before, and close to 70 Å. The maximum of about 40 Å shifts toward a lower value at 800°C.

SAXS log–log curves are represented in fig. 4. They exhibit three regions as is schematized in the same figure. AB corresponds to the limit for $q \rightarrow 0$ of the Guinier q-range; BC is the power law decay due to the internal structure of the aggregates; and CD is the Porod range related to the interfaces between primary particles. From q_B and q_C crossover points, the Debye's characteristic length, r_a, and the elementary entity size, r_θ, respectively can be obtained. These parameters are given by $r_a = \pi / q_B$ and $r_\theta = \pi / q_C$. Their values are reported in table 2.

A similitude ratio, k, can be calculated as the quotient between q_C and q_B. Then an aggregation index, N, can be defined as the r_θ size particle number which forms an r_a size aggregate

---

* IUPAC nomenclature for different hysteresis loops [14].

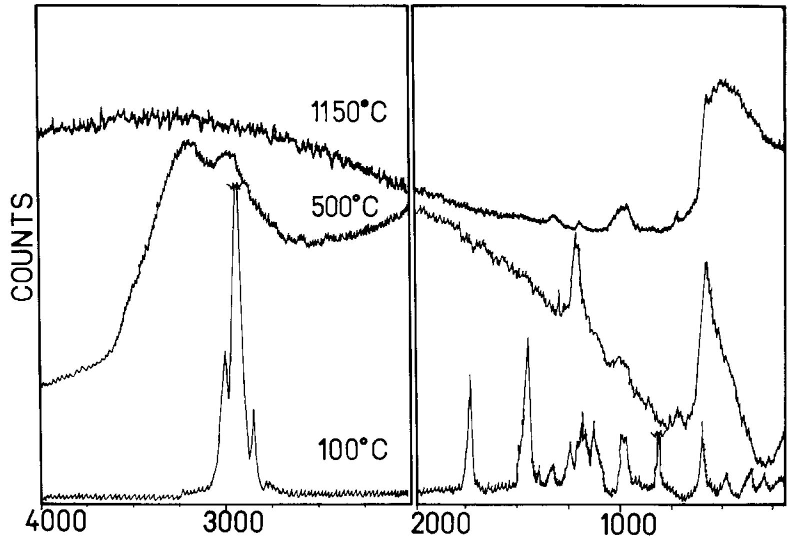

Fig. 5. Raman spectra for xerogels treated at 100°C, 500°C and 1150°C. At 500°C, the silica network began to be formed and at 1150°C a standard silica glass spectra is obtained.

that can be calculated by the expression [15]

$$N = k^3 \frac{\rho_a}{\rho_s} \qquad (2)$$

where ρ_a and ρ_s ** are the bulk and the skeletal densities of the sample respectively. The ratio ρ_a/ρ_s, the solid volume fraction, can be considered as the ratio between N times the elementary entity volume and the total volume of the aggregate.

Figure 5 compares a sequence of Raman spectra of silica xerogels after drying at 40°C and further heat treatments at 100°C, 500°C and 1150°C. Bands between 500 and 650 cm^{-1} are the well known 'defect bands' associated with small cyclic structures cyclotetrasiloxane and cyclotrisiloxane [16]. The broad band between about 3000 and 3800 cm^{-1} at 500°C corresponds to the fundamental stretching vibrations of different hydroxyl groups. It is composed of a superposition of SiO–H and Si–OH stretching vibrations. The principal change on heating is a decrease of this band indicating that the concentration of silanols is lower.

4. Discussion

A main mesopore size of 40 Å can be established along the heat treatment (fig. 3). The appearance of a second maximum pore size at 400°C may be produced when organic radicals leave the pores which happens between 230 and 330°C as is deduced from the TGA curves (fig. 1(b)). Therefore, the maximum over 70 Å is due to pores which held organic radicals ar 200°C. These larger pores produce a shrinkage of the solid disappearing at 600°C. In order to determine the relationship between r_p, V_p and S_{BET}, a cylindrical geometry for the mesopores was assumed. Under these hypotheses the mesopore radius would be

$$r_p = 2\frac{V_p}{S_{BET}}. \qquad (3)$$

Table 2 reports the pore volume, V_p, which was experimentally determined from nitrogen physisorption experiments. This volume corre-

---

** A value of vitreous silica density of $\rho_s = 2.2$ g cm^{-3} is assumed.

sponds essentially to mesopores and to a small fraction of the larger micropores. The volume occupied by micropores, V_p^*, is also given in table 2. This volume was calculated assuming the structural model of quasi-spherical aggregates of radius r_a, formed by $N+1$ primary entities of radius r_0.

The ratio between r_p, mesopore radius obtained from eq. (3), and r_a, the radius of the aggregate, permits determination of the packing type [17]. r_p/r_a values are shown in table 2. Therefore, most of these xerogels are formed by a primitive cubic packing of aggregates except sample H84, the most evolved, which has a primitive hexagonal structure.

Table 2 also shows the difference between samples prepared using different ultrasound doses. Those prepared with a high ultrasonic dose exhibit a higher similitude ratio, higher aggregation index and lower elementary entity size. For the same set, the similitude ratio and aggregation index increases with the temperature whereas the elementary entity size decreases.

Chlorination decreases xerogel viscosity [18], leading to brittle fracture of the samples. For this reason no chlorination treatment was used for sintering samples.

5. Conclusions

Silica monolithic glasses have been prepared from gels obtained by sonocatalysis and formamide as an additive, without chlorination and heat treated to 1150°C by a constant rate heating.

Structural evolution of silica xerogels during thermal treatment up to 800°C does not occur by sintering between elementary particles. The present result supports the model of an increase in the number of primary particles which build the aggregates. Temperature has an important influence on Debye length and packing type only above 800°C.

Ultrasound energy dose decreases the elementary entity size and increases the number of entities which form the aggregate. The effect of ultrasounds dose on aggregate size is not very strong.

This work has been supported by the projects MAT1022/91 of the CICYT and Junta de Andalucia (6015) in Spain and by the CNPq in Brazil.

The authors thank C. Fernández-Lorenzo for her help in the obtention of Raman spectra. The authors are indebted to Dr J.M. Rodriguez-Izquierdo for his helpful discussions and to the Group of Catalysis of the University of Cádiz for their contribution in the software for physisorption data treatment.

References

[1] R.D. Shoup, in: Ultrastructure Processing of Advanced Ceramics, ed. J.D. Mackenzie and D.R. Ulrich (Wiley, New York, 19788) p. 347.

[2] E.M. Rabinovich, J.B. MacChesney, D.W. Johnson Jr., J.R. Simpson, B.W. Meagher, F.V. DiMarcello, D.L. Wood and E.A. Sigety, J. Non-Cryst. Solids 63 (1984) 155.

[3] M. Yamane, J.B. Caldwell and D.T. Moore, in: Better Ceramics Through Chemistry II, ed. C.J. Brinker, D.E. Clark and D.R. Ulrich (Material Research Society, Pittsburgh, PA, 1986) p. 765.

[4] G.W. Scherer, J. Am. Ceram. Soc. 73 (1990) 3.

[5] J. Zarzycki, in: Ultrastructure Processing of Ceramic Glasses and Composites, ed. L.L. Hench and D.R. Ulrich (Wiley, New York, 1984) p. 27.

[6] J. Fricke, in: Aerogels (Springer, Berlin, 1987).

[7] J. Zarzycki, M. Prasas and J. Phalippou, J. Mater. Sci. 17 (1982) 3371.

[8] L.L. Hench, in: Science of Ceramic Chemical Processing, ed. L.L. Hench and D.R. Ulrich (Wiley, New York, 1986) p. 52.

[9] G. Orcel, J. Phalippou and L.L. Hench, J. Non-Cryst. Solids 104 (1988) 170.

[10] N. de la Rosa-Fox, L. Esquivias and J. Zarzycki, J. Mater. Sci. Lett. 10 (1991) 1237.

[11] N. de la Rosa-Fox, L. Esquivias and J. Zarzycki, Diff. Defect Data 53&54 (1987) 363.

[12] W.T. Thompson, Philos. Mag. 42 (1871) 448.

[13] C.J. Pierce, J. Phys. Chem. 57 (1953) 149.

[14] IUPAC Pure Appl. Chem. 57 (1985) 603.

[15] N. de la Rosa-Fox and L. Esquivias, to be published.

[16] M. Guglielmi and G. Principi, J. Non-Cryst. Solids 48 (1982) 161.

[17] R.G. Avery and J.D.F. Ramsay, J. Colloid Interf. Sci. 42 (1973) 597.

[18] G. Hetherington, K.H. Jack and J.C. Kennedy, Phys. Chem. Glasses 5 (1964) 130.